V European Conference on Computational Fluid Dynamics
ECCOMAS CFD 2010
J. C. F. Pereira and A. Sequeira (Eds)
Lisbon, Portugal,14-17 June 2010

FLUID–STRUCTURE–ACOUSTIC INTERACTION, ALGORITHMS AND IMPLEMENTATIONS USING THE FINITE ELEMENT METHOD

S. Zörner[*†], M. Kaltenbacher[*]

[*]Chair of Applied Mechatronics
Lakeside Park, Gebäude B04a
9020 Klagenfurt – Austria
e-mail: stefan.zoerner@uni-klu.ac.at
e-mail: manfred.kaltenbacher@uni-klu.ac.at
[†]Department of Sensor Technology Paul–Gordan Str. 3/5
91052 Erlangen – Germany

Key words: Finite Element Method, Fluid–Structure–Acoustic Interaction, Phonation

Abstract. *An advanced Finite Element Method is presented which is being applied to simulate fluid flow interacting with a soft structure. Furthermore, the generated sound from fluid flow and structural mechanics is also taken into account. To get a correct model for the acoustic source terms resulting from the fluid flow Lighthill's analogy is applied, while structural mechanics is coupled to acoustics via the common interface. As a result we have a coupling between fluid flow, structural mechanics and acoustics.*
While we assume the acoustics has no back reaction neither on the fluid nor on the structure, fluid and structure influence each other in a strong sense. Therefore, additionally to the non–linearity arising from the Navier–Stokes equations the strong coupling yield a further non–linearity, which needs to be tackled. Different kind of iterative algorithm can be applied to solve the problem, like the relaxation according to Aitken. A further challenge is the mesh deformation which occurs due to the movement of the structure. We apply an Arbitrary Lagrangian Eulerian (ALE) approach[1,2]. Dealing with all three physical fields, their interactions and the above mentioned difficulties is very costly concerning computational time and therefore we limit ourselves to 2d simulations.

The resulting algorithms are implemented in the research code CFS++[3] *and find its application in simulating the human phonation process, a prefect example since all mentioned physical fields and their interactions are present. Due to airflow through the trachea, generated by compression of the lungs, the vocal folds, positioned inside the larynx, start to vibrate. The vibration in turn causes the airflow to pulsate, which generates the main frequency of the human voice, the so called phonation.*

1 INTRODUCTION

In this paper a fully coupled fluid–structure–acoustic formulation is presented[4,5], which has been implemented in the research code *CFS++*. The motivation arises from the phonation process, which is not yet completely understood. Phonation is generated inside the larynx and results from fluid flow through the trachea which generates vibrations of the vocal folds. Therewith, fluid flow as well as mechanical vibrational induced sound is generated.
A sketch of the relationships between the physical fields is given in figure 1, which has been implemented using the finite element (FE) method. Generally speaking, we consider

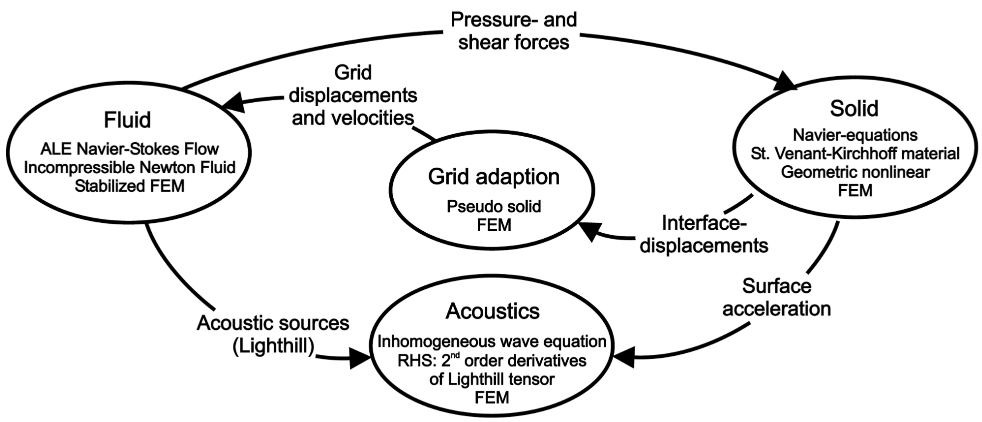

Figure 1: Sketch of interaction and coupling types between fluid mechanics, structure mechanics and acoustics.

a fluid flow which acts onto a deformable structure, which in turn influences the adhering fluid. Therefore, special boundary conditions are given at the common interface which are specified in section 2.3. Furthermore, the deforming structure prescribes the fluid domain and its grid which has to change constantly in time. An Arbitrary Lagrangian Eulerian (ALE) method is being used to tackle the problem. In section 2.4 the wave equation is presented together with the calculation of the sound sources resulting from fluid dynamics and structural mechanics.

2 PHYSICAL FIELDS

2.1 Fluid mechanics

In the case of phonation a Mach number of smaller than 0.3 is guaranteed which allows the assumption of an incompressible flow. Therefore, the fluid may be described by the incompressible Navier–Stokes equations given by the momentum and mass conservation

$$\rho_\mathrm{f}\frac{\partial \vec{v}}{\partial t} + \rho_\mathrm{f}(\vec{v}\cdot\nabla)\vec{v} + \nabla p - \mu\Delta\vec{v} = 0\,, \tag{1}$$

$$\nabla\cdot\vec{v} = 0\,. \tag{2}$$

Thereby, ρ_f is the fluid density, $\vec{v}$ the fluid velocity, p the pressure and μ the dynamic viscosity. Inflow and outflow are treated by the inhomogeneous boundary condition

$$p(\vec{x},t) = p_0(\vec{x},t) \qquad \Gamma_D \times \{0,T\} \tag{3}$$

at the interface Γ_D. A sketch of the simulation domain with its different boundaries is given in figure 2. For fixed walls the fluid adheres and the velocity is set to zero, whilst the pressure component is free. The common interface between moving structure and fluid Γ_fs is described in section 2.3. This results in three different boundary treatments, partitioning the boundary $\Gamma = \Gamma_D \cup \Gamma_\mathrm{fs} \cup \Gamma_N$ with the latter representing the fixed walls.

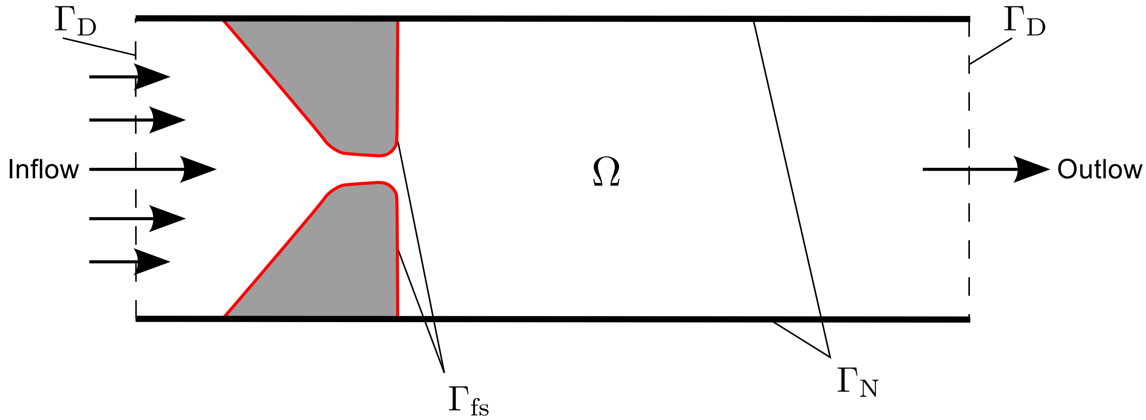

Figure 2: Sketch of simulation model for the larynx, defining the different boundaries.

2.2 Solid mechanics

The partial differential equation of solid mechanics for linear elasticity is given by Navier's equation

$$\nabla \cdot \sigma_\mathrm{s} = \rho_\mathrm{s} \frac{\partial^2}{\partial t^2} \vec{u}\,, \tag{4}$$

with the Cauchy stress tensor σ_s, the solid density ρ_s and the displacement $\vec{u}$. By introducing the tensor of elasticity $[c]$ and the tensor of linear strain $[S]$, Hook's law may be expressed by

$$\sigma_\mathrm{s} = [c][S] \tag{5}$$

and the linear strain-displacement by

$$[S] = \nabla^\mathrm{sym} \vec{u}\,. \tag{6}$$

Substituting (5) and (6) into (4) results in the final partial differential equation (PDE) for linear elasticity

$$\mathcal{B}^T[c]\mathcal{B}\vec{u} = \rho_{\mathrm{s}}\frac{\partial^2}{\partial t^2}\vec{u} \tag{7}$$

with the differential operator $\mathcal{B}$ which for the 2d plane case is

$$\mathcal{B} = \begin{pmatrix} \frac{\partial}{\partial x} & 0 \\ 0 & \frac{\partial}{\partial y} \\ \frac{\partial}{\partial y} & \frac{\partial}{\partial x} \end{pmatrix} .$$

2.3 Fluid–solid interaction

Considering the common interface Γ_{fs} between solid and fluid, fluid velocity and structural velocity needs to be identical given by

$$\vec{v} = \frac{\partial}{\partial t}\vec{u} \qquad \text{on } \Gamma_{fs} . \tag{8}$$

This implies that the fluid adheres to the structure. Furthermore, fluid stress σ_f and solid stress have to coincide in normal direction which is enforced by

$$[\sigma_{\mathrm{s}}]\cdot\vec{n} = [\sigma_{\mathrm{f}}]\cdot\vec{n} \qquad \text{on } \Gamma_{\mathrm{fs}}. \tag{9}$$

In (9) the fluid acting on the solid is equivalent to a force $\vec{f}_{\mathrm{fs}}$ which may be split into a pressure and a shear component

$$\vec{f}_{\mathrm{fs}} = \rho_{\mathrm{f}} \underbrace{\int\limits_{\Gamma_{\mathrm{fs}}} -pI\cdot\vec{n}\,\mathrm{d}x}_{\text{pressure}} + \underbrace{\int\limits_{\Gamma_{\mathrm{fs}}} \mu\left(\nabla\vec{v} + (\nabla\vec{v})^T\right)\cdot\vec{n}\,\mathrm{d}x}_{\text{shear}} \ .$$

2.4 Acoustics

In our application the acoustic calculation domain coincides with the fluid domain Ω, where the acoustic pressure propagation is described by the wave equation, which in index notation is given as

$$\frac{1}{c^2}\frac{\partial^2 p'}{\partial t^2} - \frac{\partial^2 p'}{\partial x_i^2} = \frac{\partial^2 T_{ij}}{\partial x_i \partial x_j} \tag{10}$$

with the speed of sound c, p' the acoustic pressure and $\mathbf{T}$ the Lighthill tensor

$$T_{ij} = \underbrace{\rho_f v_i v_j}_{\text{Reynolds stress}} + \underbrace{\tau_{ij}}_{\text{Viscous stress}} + \underbrace{\left[p' - c^2\rho'\right]\delta_{ij}}_{\text{Heat conduction}} . \tag{11}$$

In (11) ρ' is the acoustic density . For high Reynolds number the viscous stress may be neglected[6,7]. The heat conduction may also be neglected since in regions of ambient temperature the contribution of heat conduction is of the same order as the viscous term. This leads to the approximation

$$T_{ij} \approx \rho_{\mathrm{f}} v_i v_j \ . \tag{12}$$

The fluid induced sound is a sound source given on the whole domain Ω. Additionally, at the structure interface Γ_{fs} vibrational induced sound is enforced by

$$\frac{\partial}{\partial t}\vec{u} \cdot \vec{n} = \vec{v}_a \cdot \vec{n} \qquad \text{on } \Gamma_{\mathrm{fs}} \tag{13}$$

setting the structural and acoustic velocity $\vec{v}_a$ equal in normal direction. With the linearised momentum equation for acoustics

$$\frac{\partial}{\partial t}\vec{v}_a \cdot \vec{n} = -\frac{1}{\rho_{\mathrm{f}}}\frac{\partial}{\partial n}p' \qquad \text{on } \Gamma_{\mathrm{fs}} \tag{14}$$

the source terms in pressure formulation is

$$\frac{\partial}{\partial n}p' = -\rho_{\mathrm{f}}\frac{\partial^2}{\partial t^2}\vec{u} \cdot \vec{n} \qquad \text{on } \Gamma_{\mathrm{fs}} \ . \tag{15}$$

For the considered case we assume, that there is no back reaction of the acoustic onto the vibrating solid.

3 FINITE ELEMENT FORMULATION

3.1 Fluid mechanics (FE)

To employ the FE method, the weak form of the PDE is regarded, which is then approximated by appropriate set of functions. In this section a sketch is only presented, for a detailed view we refer to appropriate literature[8]. We define the scalar product as

$$(p, q) = \int_{\Omega_{\mathrm{f}}} pq \, \mathrm{d}\Omega \ .$$

Hence the weak form of (2) is

$$\left(\dot{\vec{v}}, \vec{w}\right) + \left(\vec{v}_{\mathrm{c}} \cdot \nabla \vec{v}, \vec{w}\right) - \left(p, \nabla \cdot \vec{w}\right) + \nu\left(\nabla \vec{v}, \nabla \vec{w}\right) - \left(\nabla \cdot \vec{v}, q\right) = \left(\vec{h}, \vec{w}\right)_{\Gamma_{\mathrm{f}}} \tag{16}$$

with $\vec{h}$ representing the boundary conditions. The pressure is approximated by

$$p \approx p_h := \sum_{i \in N} p_i(t)\varphi(\vec{x}),$$

which is also done for the test function and the velocity field. Additionally applying the BDF2-scheme to the unsteady flow problem we get the final algebraic system of equations

$$\left[\mathbf{M} + \frac{2}{3}\triangle t\mathbf{N}\right]\mathbf{v}^{n+1} + \frac{2}{3}\triangle t\mathbf{G}\mathbf{p}^{n+1} = \mathbf{M}\left(\frac{4}{3}\mathbf{v}^n - \frac{1}{3}\mathbf{v}^{n-1}\right) \ . \tag{17}$$

The Streamline Upwind Petrov Galerkin[9,10,11] (SUPG) was used as a residual based stabilisation, but will not be covered here.

3.2 Structure mechanics (FE)

Regarding structural mechanics, the weak form reads as

$$\left([c]\mathcal{B}\vec{u}, (\mathcal{B}\vec{w})^T\right) = \rho_\mathrm{s}\left(\ddot{\vec{u}}, \vec{w}\right) \tag{18}$$

resulting in the following semi-discrete Galerkin formulation

$$\mathbf{M}\ddot{\mathbf{u}} + \mathbf{K}\mathbf{u} = 0 \tag{19}$$

with $\ddot{\mathbf{u}}$ denoting the second derivative in time. The time discretisation is performed by the standard implicit Newmark scheme.

3.3 Acoustics (FE)

For the acoustics, equation (10) is multiplied by an appropriate test function q and integrated over the domain Ω resulting in

$$\left(\frac{1}{c^2}\frac{\partial^2 p'}{\partial t^2} - \frac{\partial^2 p'}{\partial x_i^2} - \frac{\partial^2 T_{ij}}{\partial x_i \partial x_j}, q\right) = 0 \; . \tag{20}$$

Applying the integral theorem of Green to the spatial derivative we get

$$\left(\frac{\partial^2 p'}{\partial x_i^2}, q\right) = \left(\frac{\partial p'}{\partial \vec{n}}, q\right)_\Gamma - \left(\frac{\partial p'}{\partial x_i}, \frac{\partial q}{\partial x_i}\right) \tag{21}$$

whereby the additional boundary integral arises. At the boundaries where the computational domain adjoins to a fixed structure, hard reflecting walls are employed resulting in homogeneous Neumann boundary conditions for Γ_fs and Γ_N. For in- and outflow it has to be guaranteed that any wave impinging the boundary leaves the computational domain and does not reflect back. A first order absorbing boundary[8] is used, expressed by

$$\frac{\partial p'}{\partial \vec{n}} = -\frac{1}{c}\frac{\partial p'}{\partial t} \; . \tag{22}$$

Analogously the integration by parts is applied to the term including the Lighthill tensor, resulting in

$$\left(\frac{\partial^2 T_{ij}}{\partial x_i}\partial x_j, q\right) = \left(\frac{\partial T_{ij}}{\partial x_j} n_i, q\right)_\mathrm{fs} - \left(\frac{\partial T_{ij}}{\partial x_j}, \frac{\partial q}{\partial x_i}\right) \; . \tag{23}$$

The boundary term may be substituted based on the continuity equation[12] by

$$\left(\frac{\partial T_{ij}}{\partial x_j} n_i, q\right)_\mathrm{fs} = -\left(\frac{\partial p'}{\partial n_i}, q\right)_\mathrm{fs} - \left(\frac{\partial \rho_\mathrm{f} v_i}{\partial t} n_i, q\right)_\mathrm{fs} \; . \tag{24}$$

The last term in (24) vanished for a fixed boundary. For vibrating structures we use (15), which together with (22) changes (10) to

$$\begin{aligned}\left(\frac{1}{c^2}\frac{\partial^2 p'}{\partial t^2}, q\right) + \left(\frac{\partial p'}{\partial x_i}, \frac{\partial q}{\partial x_i}\right) \quad + \quad & \underbrace{\left(\frac{1}{c}\frac{\partial p'}{\partial t}, q\right)_{\Gamma_D}}_{\text{Absorbing boundary}} \quad = \\ - \quad & \underbrace{\left(\frac{\partial T_{ij}}{\partial x_j}, \frac{\partial q}{\partial x_i}\right)}_{\text{Flow–induced sound}} - \underbrace{\left(\rho_\mathrm{f}\frac{\partial^2 u_i}{\partial t^2} n_i, q\right)_{\mathrm{fs}}}_{\text{Vibrational–induced sound}} \quad . \end{aligned} \tag{25}$$

This in turn yields the following semi-discrete Galerkin formulation

$$\mathbf{M}\ddot{\mathbf{p}}' + \mathbf{D}\dot{\mathbf{p}}' + \mathbf{K}\mathbf{p}' = \mathbf{F}\ , \tag{26}$$

which in turn is discretsed in time again by the standard implicit Newmark scheme.

4 APPLICATION TO HUMAN PHONATION

4.1 Human phonation model

The simulation setup to model the human larynx consists of a channel with the two vocal folds[13] which act as a constriction inside the channel. The setup is sketch in figure 3 also giving insight into the mesh around the vocal folds. Approximately 45000 quadratic elements are used to resolve the fluid which results in about 400000 degrees of freedom. For structural mechanics the vocal folds have been divided into three different layers, the body, the ligament and the cover. Each have different elasticity modulus to model the real physiology more accurately. For body, ligament and cover the elasticity moduli were set to 21, 33 and 12 kPa respectively. To simulate the pressure the lungs build up a pressure gradient from in– to outflow of 1.5 kPa is regarded.

4.2 Results

The simulation show the typical movement of the vocal folds during phonation, which is divided into the divergent (opening) and convergent (closing) phase. In figure 5 the fluid field can be seen at time step 7.25 ms. The jet attached itself to the upper vocal fold is known as the Coanda effect. In our transient simulation one can see how the jet is stochastically pulled towards either side of the trachea wall.

4.3 Fluid induced and vibrational induced sound

The simulation code CFS++ is capable of separately computing the aeroacoustic disregarding the vibrational induced sound and separately calculating the acoustic propagation with the structural vibration as a sound source. In a series of simulations the acoustic field of vibrational and fluid induced sound was compared. As can be seen in figure 6a the

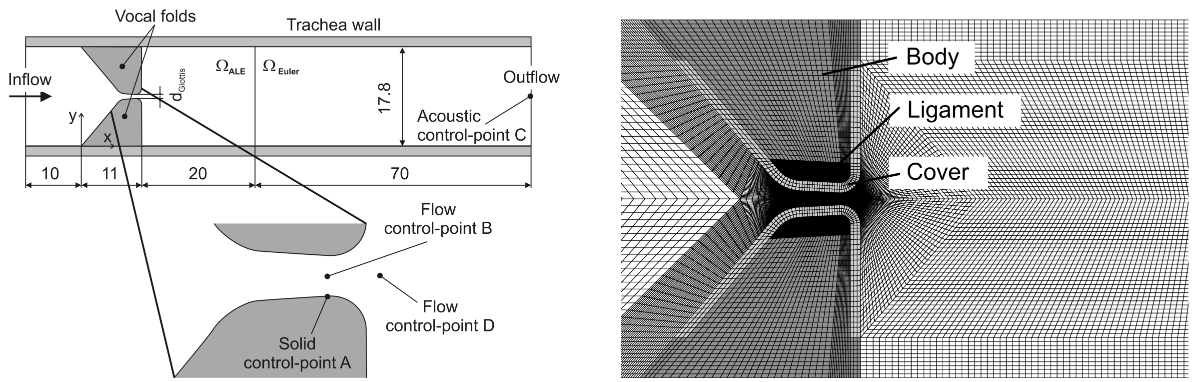

(a) Simulation model (dimensions in) mm (b) Mesh around the vocal folds

Figure 3: Model of the larynx with vocal folds and the according mesh used for the simulations.

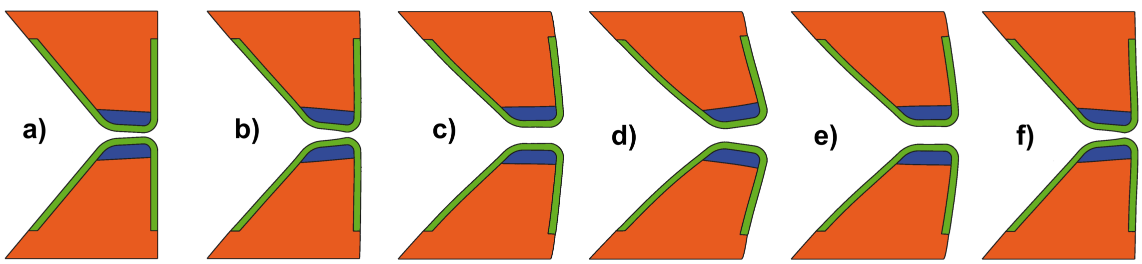

Figure 4: Computed deformation cycle of the vocal folds, which can be divided in divergent to convergent phase.

mechanical induced sound is much smaller than that of the fluid induced sound. Comparing this result with a simulation were the glottis width is enlarged to 0.7 mm (see figure 6b) it shows that the bigger glottis results in a much broader acoustic frequency spectrum. Furthermore, no dominant frequency component is recognisable as in figure 6a at about 190 Hz.

These results imply the importance of a proper closing glottis for a clear and healthy voice. Furthermore, they show that the fluid flow is the dominant source of the phonation which is hard to proof by measurements.

5 CONCLUSIONS

A method was presented and implemented to simulate fluid–structure–acoustic interaction. The scheme has been applied to investigate the human phonation process. Realistic self sustained oscillations of the vocal folds, which are induced by the fluid flow, were observed. Furthermore, the separation of fluid induced sound and vibrational induced sound made it possible to show that the dominant sound sources is the fluid flow.

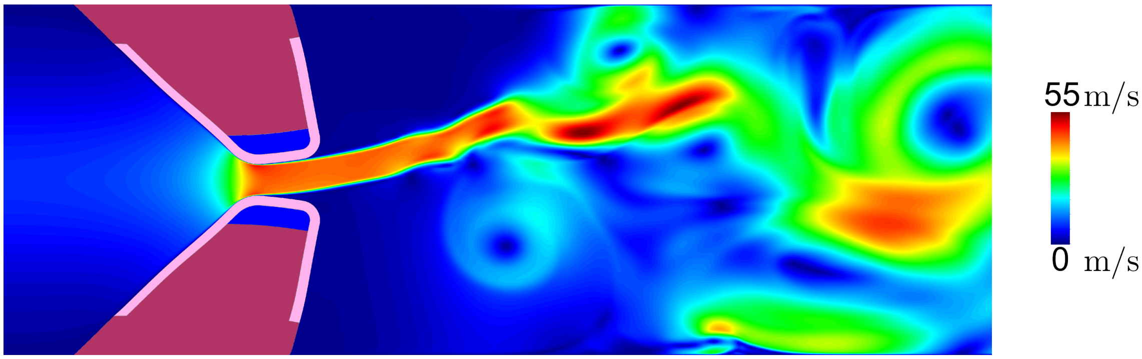

Figure 5: Snap–shot of velocity field and deformation of vocal folds. Jet is attached to the top vocal fold — Coanda effect.

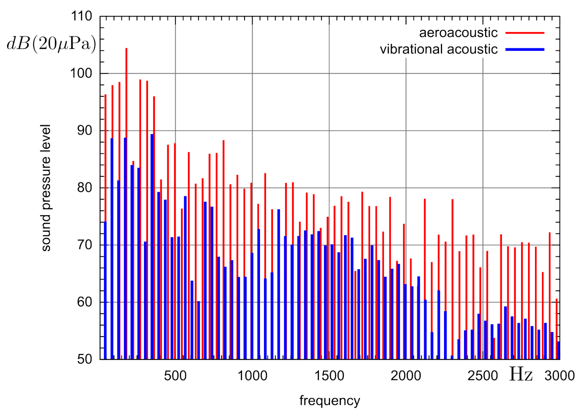

(a) Acoustic spectra of vibrational and fluid induced sound at a glottis width of 0.3 mm

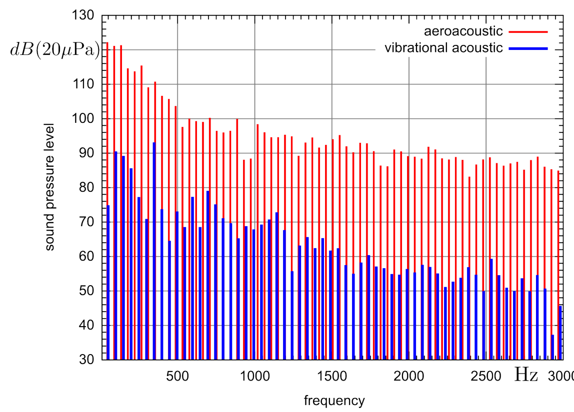

(b) Acoustic spectra of vibrational and fluid induced sound at a glottis width of 0.7 mm

Figure 6: Comparison of acoustic spectra for fluid induced and vibrational induced sound simulation for different glottis widths.

6 ACKNOWLEDGEMENTS

This work was supported by Deutsche Forschungsgemeinschaft Grant No. FOR894/1 *Strömungsphysikalische Grundlagen der menschlichen Stimmgebung*.

REFERENCES

[1] C. W. Hirt, A. A. Amsden, and J. L. Cook. An arbitrary lagrangian-eulerian computing method for all flow speeds. *Journal of Computational Physics*, 14(3):227 – 253, 1974.

[2] T. J. R. Hughes, W. K. Liu, and T. K. Zimmermann. Lagrangian-eulerian finite element formulation for incompressible viscous flows. *Computer Methods in Applied*

Mechanics and Engineering, 29(3):329 – 349, 1981.

[3] CFS++: Coupled Field Simulation Applied Mechatronics — University Erlangen, Institute of Sensor Technology — University Erlangen *Technical Report*, 2010.

[4] G. Link. *A Finite Element Scheme for Fluid-Solid-Acoustics Interactions and its Application to Human Phonation*. PhD thesis, Technisch Fakultät Universität Erlangen-Nürnberg, 2008.

[5] G. Link, M. Kaltenbacher, M. Breuer, and M Döllinger. A 2d finite-element scheme for fluid-solid-acoustic interactions and its application to human phonation. *Computer Methods in Applied Mechanics and Engineering*, 198:3321–3334, 2009.

[6] M. J. Lighthill. On sound generated aerodynamically I. General theory. *Proceedings of the Royal Society of London*, 211:564–587, 1951.

[7] M. J. Lighthill. On sound generated aerodynamically II. Turbulence as a source of sound. *Proceedings of the Royal Society of London*, 222:1–32, 1953.

[8] M. Kaltenbacher. *Numerical Simulation of Mechatronic Sensors and Actuators.* Springer, Berlin, 2. edition, 2007. ISBN: 978-3-540-71359-3.

[9] T. E. Tezduyar, S. Mittal, S. E. Ray, and R. Shih. Incompressible flow computations with stabilized bilinear and linear equal-order-interpolation velocity-pressure elements. *Computer Methods in Applied Mechanics and Engineering*, 95(2):221 – 242, 1992.

[10] Leopoldo P. Franca, Sergio L. Frey, and Thomas J. R. Hughes. Stabilized finite element methods: I. application to the advective-diffusive model. *Computer Methods in Applied Mechanics and Engineering*, 95(2):253 – 276, 1992.

[11] Leopoldo P. Franca and Charbel Farhat. Bubble functions prompt unusual stabilized finite element methods. *Computer Methods in Applied Mechanics and Engineering*, 123(1-4):299 – 308, 1995.

[12] M. Kaltenbacher and M. Escobar and M. I. Ali and S. Becker Numerical Simulation of Flow-Induced Noise Using LES/SAS and Lighthill's Acoustics Analogy *International Journal for Numerical Methods in Fluids*, doi: 10.1002/fld.2123 2009

[13] S.L. Thomson, L. Mongeau, and S.H. Frankel. Physical and numerical flow-excited vocal fold models. In *3rd International Workshop MAVEBA*, pages 147–150. Firenze University Press, 2003. ISBN 88-8453-154-3.